

Helium Ignition in the Cores of Low-Mass Stars

Alfred Gautschy, CBmA Liestal and ETH-Bibliothek Zürich
November 27, 2024

In stars with $M_* \lesssim 2M_\odot$, nuclear burning of helium starts under degenerate conditions and, depending on the efficiency of neutrino cooling, more or less off-center. The behavior of the *centers* of low-mass stars undergoing core helium ignition on the $\log \rho - \log T$ plane is not thoroughly explained in the textbooks on stellar evolution and the appropriate discussions remain scattered throughout the primary research literature. Therefore, in the following exposition we collect the available knowledge, we make use of computational data obtained with the open-source star-modeling package MESA, and we compare them with the results in the existing literature. The line of presentation follows essentially that of Thomas (1967) who was the first who outlined correctly the stellar behavior during the off-center helium flashes that lead to central helium burning. The exposition does not contain novel research results; it is intended to be a pedagogically oriented, edifying compilation of pertinent physical aspects which help to *understand* the nature of the stars.

SHORTLY AFTER HENYEY'S METHOD CAME INTO USE to solve numerically the equations of stellar structure and evolution, model stars were followed up the first giant branch and into core helium burning (Härm & Schwarzschild 1964). In these early computations, helium ignited in the stars' very centers because neutrino cooling was not yet accounted for. In his PhD thesis, Thomas (1967)¹ computed the evolution of a $1.3M_\odot$ star from the ZAMS to the beginning of core helium burning and, in contrast to the earlier Schwarzschild & Härm calculations, added neutrino energy losses. The energy leak in the stellar core induced by the weakly interacting neutrinos leads to an important, qualitative change in central stellar structure: Instead of a monotonous temperature drop from the center, a temperature inversion develops in the deep interior. Because of the strong temperature dependence of the nuclear reaction rates, helium burning starts off-center with the nuclear-active shell eating slowly its way to the star's center.

The paper of Demarque & Mengel (1971) contains results from stellar-evolution computations of low-mass population II stars ranging in mass from 0.5 to $0.85M_\odot$. The authors aimed at investigating the critical core mass at which helium ignites and the subsequent evolutionary phase with its core cooling. Accordingly, the paper contains a figure showing, on the $\log \rho - \log T$ plane, the loci of stellar centers under different physical conditions; in particular, one plot shows the central cooling and expansion episode during the initial helium flash. Not the complete evolution from the top of the giant branch to the

This document is best indulged electronically.

CBmA: Center for Basement Astrophysics; an autonomous astronomy research venture of the same mindset as cbastro.org

¹ The ZfA paper is essentially a verbatim reproduction of the thesis.

arrival of the star model on the horizontal branch was computed so that the loci on the $\log \rho - \log T$ plane remained incomplete.

At around the same time, Mengel & Sweigart (1981) and Despain (1981) published papers wherein they painstakingly computed the evolution of a low-mass Population II star from the top of the giant branch, through the helium flashes, onto the horizontal branch (an $0.7M_{\odot}$ star with 8 thermal pulses of the He shell in the Mengel & Demarque paper and an $0.6M_{\odot}$ star with 12 thermal pulses in the paper of Despain). Mengel & Sweigart (1981) illustrated the evolution during the thermal-pulse episode with detailed diagrams for luminosity, and temperature. A time – mass diagram (lately referred to as Kippenhahn diagram) tracing the extent of convection zones and the locations of nuclear burning regions documented the closing in on the stellar center of the thermally unstable helium-burning shell on the time-scale of the order of a million years.

Despain (1981) emphasized that his stellar evolution computations of a $0.5M_{\odot}$ Pop II star did not resort to any artificial shifting of the thin hydrogen-burning shell in the discretized model star during its evolution along the giant branch. Therefore, he considered his computations as a benchmark for older ones to scrutinize their results, which were obtained with then unproven numerical simplifications. Despain went on to explain the model star’s structural behavior on its way starting from the ZAMS to the onset of thermal pulses on the lower AGB. In particular, Despain put forth physical explanations of numerical findings during the off-center onset of He burning and the inward evolution of the He-burning shell. Establishing a local stability analysis; he explained the thermal instability of the helium shell, which underwent 12 thermal pulses before core helium burning established itself, and he also presented a $\log \rho - \log T$ diagram showing the locus of the star’s center and of the temperature maximum during the star’s evolution from the top of the giant branch to the horizontal branch. Most importantly, Despain indicated that the star’s center moves, due to its expansion and cooling, towards the lower left of the $\log \rho - \log T$ diagram, whereas the location of maximum temperature heats at essentially constant density until the temperature maximum enters a sufficiently low-degeneracy region to also expand and hence decrease its density and also slightly its temperature. Together with the Despain & Scalo (1976) paper, Despain provided at the time the most thorough discussion and physical explanations of the mechanical and thermal behavior and the stability properties of cores of low-mass stars during the onset of helium burning in their cores. Nonetheless, the loci on the $\log \rho - \log T$ plane remained fragmentary: Only the initial He-flash phase was covered.

To the best of the author’s knowledge, the numerically established

loci of the low-mass stars' centers on the $\log \rho - \log T$ plane as already published in Demarque & Mengel (1971) or Despain (1981) never made it into textbooks on stellar structure and evolution. The œuvre of Kippenhahn & Weigert (1994), a benchmark for advanced textbooks on stellar physics, never discusses the locus of the low-mass star's center during He ignition; the authors referred to the data of Thomas (1967) but content themselves with showing the behavior of the He-ignition mass shell on the $\log \rho - \log T$ plane. Later in the book, when discussing the evolution of the central region (§ 33.4), Kippenhahn & Weigert relied on a plot of Iben (1974) wherein the loci of the centers of stars with degenerate cores are plotted *incorrectly* for the phase of helium ignition. Even in the most recent texts on stellar evolution, the situation has not improved; e.g. in Salaris & Cassisi (2005, their Fig. 5.12) the locus of the $1M_{\odot}$ star's center evolution on the $\log \rho - \log T$ plane continues to be plotted incorrectly.

Until recently, only a few specially tuned stellar evolution codes could reliably evolve low-mass model stars up the first giant branch and the ensuing onset of the helium burning either onto the horizontal branch or into the clump giant region of the HR Diagram. Following the ever narrowing hydrogen burning shell during the evolution up along the giant branch either requires a huge number of timesteps to accurately follow the evolution of the nuclear burning shell. To circumvent the problem, elaborate transport prescriptions to shift the H-burning shell artificially were implemented at the time when computers were much slower than today, this allowed to maintain big enough timesteps and hence reduced the computational load considerably. Furthermore, once helium burning ignites, the timesteps can easily shrink to a fraction of a day; this after starting the evolution of the model star with temporal step-widths of the order of several 10^8 yrs. Hence, the numerics of stellar evolution codes, which have to cope with this huge temporal resolution range, needs to have appropriately robust discretization schemes. Frequently, shortcuts on to the horizontal branch were taken by the modelers; they evolved low-mass stars up the giant branch, till shortly before the onset of He burning. Then, by suitably modifying the numerical models, the stars were forced onto the horizontal branch so that the full stellar evolution computations could be resumed there. The paper of Serenelli & Weiss (2005) discussed and compared various methods which were applied in the past.

To gather information on mixing in the deep interior of very metal-poor low- and intermediate-mass stars, Suda & Fujimoto (2010) evolved their models from the main sequence to the thermally-pulsing AGB. Suda & Fujimoto showed a $\log \rho_c - \log T_c$ diagram with *complete* loci as traced out by the centers low-mass star models; the

properties of the loci were, however, only mentioned en passant in the text without any deeper explanation.

Already at the end of the very first computation of a core helium flash, Härm & Schwarzschild (1964) addressed the question if the ignition episode could be a dynamical one. Subsequently this aspect generated a considerable body of literature, a body which continues to grow to the present. The current opinion arrived at from multidimensional CFD simulations is that the star remains essentially in hydrostatic equilibrium during the helium ignition process. The complex and dynamically changing convection zone in the helium-burning layer gives, however, rise to potential elemental mixing that cannot be captured with the simplified and canonically applied mixing-length model of convection in the conventional stellar-evolution approaches. The paper of Mocák et al. (2011) gives an impression of the current state of information and can serve as a guide to the literature on the fluid dynamical aspects of the ignition of core helium burning.

As a by-product of the exoplanet search of the *Kepler* spacecraft mission, a huge number of stars in a selected field in the sky got highest-precision time-series photometry. Among them are also red giants exhibiting stochastically driven oscillations whose frequencies let us probe the otherwise inaccessible internal structure (see e.g. Bedding et al. 2011). In particular, the oscillations whose restoring force have a buoyancy contribution grant access to the regions that are influenced by nuclear burning; i.e. these modes can probe a red giant's stage of evolution: they allow to discriminate between stars being still along the first giant branch, those being just during the onset of core helium burning, and the stars already being during central helium burning. It appears that for the first time we see now observational evidence of stars that are in the process of igniting helium in their cores (Bildsten et al. 2012).

The fast present-day personal computers and the advent of a new generation of stellar evolution codes, in particular the MESA collection (Paxton et al. 2011), proved to be capable to evolve low-mass stars into helium core burning even without artificially shifting narrow H-burning shells during the first giant-branch evolution or skipping the off-center helium flashes. Hence, it is now possible to study extensively and in detail even with modest computer-hardware infrastructure the behavior of stars during the relatively short-lived initial off-center helium burning in a shell and its subsequent evolution toward the star's center.

THIS EXPOSITION IS GOING TO REMIND THE READER OF OLD KNOWLEDGE – the first of it put forth almost half a century ago. No new science is going to be unearthed; old facts from the key-papers referred

to above are collected, newly arranged, and freshly illustrated so that hopefully, after this new iteration, the correct loci on the $\log \rho - \log T$ plane of the centers of helium-igniting low-mass stars will eventually find their way into the upcoming generations of textbooks on stellar physics.

Numerical modeling

All the data to which the ensuing discussion will refer were obtained with the versatile MESA code suite, which is comprehensively described in Paxton et al. (2011). The computations were performed using release version 3251. Since we are only interested in the generic behavior of the model stars, we kept the prescription of the physical ingredients as simple as possible. Hence, except if mentioned explicitly otherwise in the text, we computed the stellar-evolution models without rotation, magnetic fields, and we neglected mass loss. Convection was treated according to Henyey’s MLT prescription and we adopted the Schwarzschild criterion for convective instability; the mixing-length was set ad hoc to 1.8 pressure scale-heights.

Even though different microphysics and in particular more appropriate treatment of dynamical convection will change the results quantitatively, probably mainly with respect to abundance profiles and the associated consequences, we are positive that the following discussion caught the generic nature of low-mass stars’ evolution through the onset of core helium burning and – viewed on the HR diagram – their relatively fast transition from the top of the giant branch onto the horizontal branch or into the clump on the giant branch.

Low-mass stellar evolution to the onset of helium burning

In the following, talk of ‘low-mass stars’ shall refer to stars whose core helium burning starts under degenerate conditions. Since neutrino cooling usually causes the maximum of temperature to be reached off-center, helium burning too starts off-center. Eventually, the *central* helium-burning stage is reached through a series of thermal pulses of the inwardly propagating helium-burning shell; during this process, the centers of low-mass stars trace a generic path on the density – temperature plane, the characteristics of which lies at the center of attention in this exposition.

Figure 1 shows two representative evolutionary tracks of a $1.3M_{\odot}$ (heavy line) and a $2.1M_{\odot}$ star (thin line) as computed with MESA. For the discussion of the off-center onset of helium burning under degenerate conditions we chose the $1.3M_{\odot}$ case because it was historically

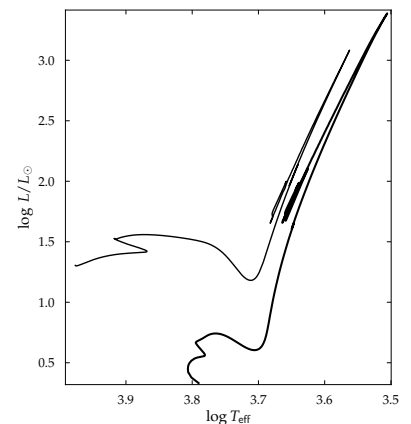


Figure 1: Conservative evolution up to central helium burning, traced out in the HR Diagram of a $1.3M_{\odot}$ and a $2.1M_{\odot}$ star, respectively, both initially with the abundances $X = 0.70, Z = 0.02$.

the first one for which the off-center He-flash and the ensuing secondary flashes were presented (Thomas 1967). The star with $2.1M_{\odot}$ in Fig. 1 was chosen because its mass just marginally exceeds the critical stellar mass above which helium burning ignites in the center and under only weakly degenerate conditions; the difference of the nuclear evolution is not visible in the track on the HR plane but it is evident on the $\log \rho_c - \log T_c$ plane

The evolution of the model stars, which are discussed in the following, was computed in quasi-hydrostatic fashion through core hydrogen burning, and then into central helium burning until central helium abundance dropped to $Y_c = 1 \cdot 10^{-4}$. The computations started with chemically homogeneous ZAMS models assuming $X = 0.7, Z = 0.02$.

The initial off-center helium flash

Once a low-mass star reaches the top of the giant branch (e.g. as shown in Fig. 1) the maximum temperature is going to exceed the critical level of about 10^8 K above which helium starts to fuse mostly into ^{12}C via the 3α reaction. The maximum temperature of the low-mass stars is attained not in the center but at a mass depth that depends on the total stellar mass and on the specific microphysics – foremost on the efficiency of the neutrino energy-losses. The particular numbers that will be referred to throughout this exposition are prone to change depending on the particular realization of the microphysical processes included in the evolution computations and on particular choices of the stars. The qualitative nature of the stellar behavior will, however, remain unchanged and it is this *qualitative picture* that is the heart of the present story and that serves us well enough to understand the stellar behavior.

Table 1 lists a few characteristic stellar quantities for $1.3M_{\odot}$ star models during the initial helium flash. The first column lists the model numbers to which the text and the figures refer to occasionally. The second column contains the age in years of the model stars counted relative to the maximum of the initial helium flash, which was encountered at $t_0 = 4\,522\,060\,464.5$ yrs² for the chosen parameters of the evolution computation. The third column lists the radii of the models, followed by the total stellar luminosity and the contributions by helium and hydrogen burning.

The schematic structure of the stellar model at maximum helium burning (model no. 13025, at $t^* = 0$) of the initial helium flash is sketched and labeled in Fig. 2. The convective envelope and the convective shell overlying the helium-burning shell are hinted at with open circles. Nuclear burning regions, on the other hand, are hinted

² The at first sight senseless accuracy of such an epoch statement can be justified in the context of *relative* timing (i.e. $t^* = t - t_0$), which is helpful to describe the temporal evolution of the onset of core helium burning. For an absolute timing, it is sufficient to remember that it takes an $1.3M_{\odot}$ star about 4.5 Gyrs to the top of the first giant branch.

Model no.	t^*/yrs	$\log R_*/R_\odot$	$\log L_*/L_\odot$	$\log L_{\text{He}}/L_\odot$	$\log L_{\text{H}}/L_\odot$
12 850	-5033.59	2.204	3.38	1.41	3.38
12 950	-0.45	2.204	3.38	6.45	3.28
13 000	-0.01	2.204	3.38	8.55	2.91
13 025	0	2.204	3.38	9.25	2.04
13 050	0.01	2.204	3.38	8.85	0.88
13 100	0.08	2.204	3.38	7.75	-0.96
13 200	6.73	2.201	3.38	5.44	-3.66
13 500	996.71	1.823	2.84	2.96	-1.33
13 700	9 542.92	1.406	2.23	-0.09	0.30
13 900	105 296.80	1.296	2.07	-0.26	-2.70
13 984	185 217.60	1.304	2.07	4.23	-0.30

at with small black dots. In the graphical representation, the geometry is not to scale; appropriate physical quantities at selected locations are listed on the bottom of the plot, giving the masses, the radii and the corresponding temperatures, $T_6 \equiv (T/K)/10^6$ at the selected boundaries. A nuclear burning region was considered as such if the energy generation rate exceeded 100 erg/g/s.

Table 1: Selected global quantities of $1.3M_\odot$ models during the initial helium flash cycle, which is discussed in detail in the text.

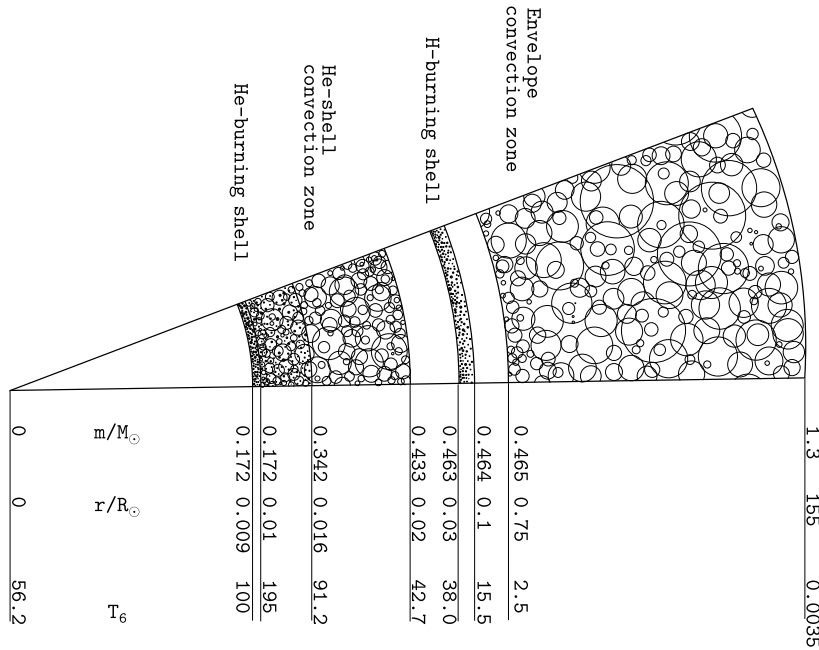


Figure 2: Schematic internal structure of a star model at maximum nuclear energy release during the initial helium flash. The scales of the radiative, convective, and nuclear burning regions are not constant through the sketch. Numerical values of selected physical quantities, adopted from model number 13 025, are tabulated on the bottom.

At model 12 850, the luminosity generated in the hydrogen-burning shell is still producing essentially the total stellar luminosity; at this epoch, i.e. at about $t^* \approx -5034$ yrs, the helium shell contributes roughly one percent to the total luminosity. Within the ensuing roughly 5000 yrs, the helium luminosity grows by roughly eight orders of magnitude. When the temperature exceeds the limit for the

onset of 3α burning off-center, the peak of the symmetric temperature bump lies at about $0.174M_{\odot}$ (see model number 12 850 in Fig. 3). The density at the temperature maximum does not change significantly during the onset of the initial flash (see the red line connecting $m = 0.174M_{\odot}$ in Fig. 3), all of the generated energy goes into further rising the temperature.³

Applying the energy equation to the steep temperature wall the develops during the helium flash at the inner edge of this nuclear burning shell

$$\partial_m L \approx -c_V \partial_t T,$$

the inward propagation speed of the wall can be estimated as

$$|L| \tau \approx c_V \left| \frac{\Delta T}{\Delta m} \right| |\Delta m|^2.$$

For a given extension in mass, Δm , and a given generated luminosity, L , the magnitude of the temperature gradient, $\Delta T / \Delta m$, determines the timescale of propagation, τ , of the temperature pulse. Plugging numerical data from the evolutionary models into the above estimate shows that the temperature wall does essentially not move in mass during the initial flash. Despite the low values of the opacity⁴ in the inert stellar core, the prevailing temperature gradient is much too low there to transport energy from the flash region to the center. Therefore, only through the propagation of the temperature wall towards the stellar center does energy penetrate the inert core.

Once helium burning ignites off-center, the energy sink due to neutrinos is quickly rendered irrelevant by the encountered magnitudes of nuclear energy generation and the involved thermal energetics (see also Fig. 4). Hence, *neutrino losses are essential to set the mass depth where helium burning ignites, but they do not influence the energetics of the helium flash itself.*

As the flash gains strength, convection sets in once a critical temperature gradient, ∇T , is exceeded on the outer flank of the temperature bump. Since $\nabla T < 0$ on the lower-mass flank, the stratification there is always stable against convection, hence the peak becomes asymmetric. The inner edge of the He-shell convection zone lies close to the maximum of the 3α energy generation and it extends well into the intershell region. At the phase of maximum extension, at $t^* \approx 16$ yrs, the convection zone reaches out to about $0.455M_{\odot}$; this is still sufficiently below the inner edge of the envelope convection zone (at $0.465M_{\odot}$ as noted in Fig. 2), and separated by the hydrogen-burning shell so that under ‘normal’ burning conditions (i.e. PopI or PopII conditions) no merging of the two respective convection zones and hence no mixing was ever observed in simulations. The strong entropy jump at the hydrogen-burning shell efficiently pre-

³ This is exactly the process associated with the thermal instability of thin nuclear-burning shells in degenerate matter as encountered in thermally pulsing AGB stars. The instability is well documented and explained in standard textbooks on stellar astrophysics (e.g. Kippenhahn & Weigert 1994)

The magnitude of τ , to shift the temperature flank by its own mass thickness, varies between a few hundred seconds at flash peak (model 13 025) and many thousand years once the helium-burning shell stabilizes again.

⁴ Opacity ranges from about $0.1 \text{ cm}^2/\text{g}$ close to the helium shell to about $0.01 \text{ cm}^2/\text{g}$ in the strongly degenerate stellar center.

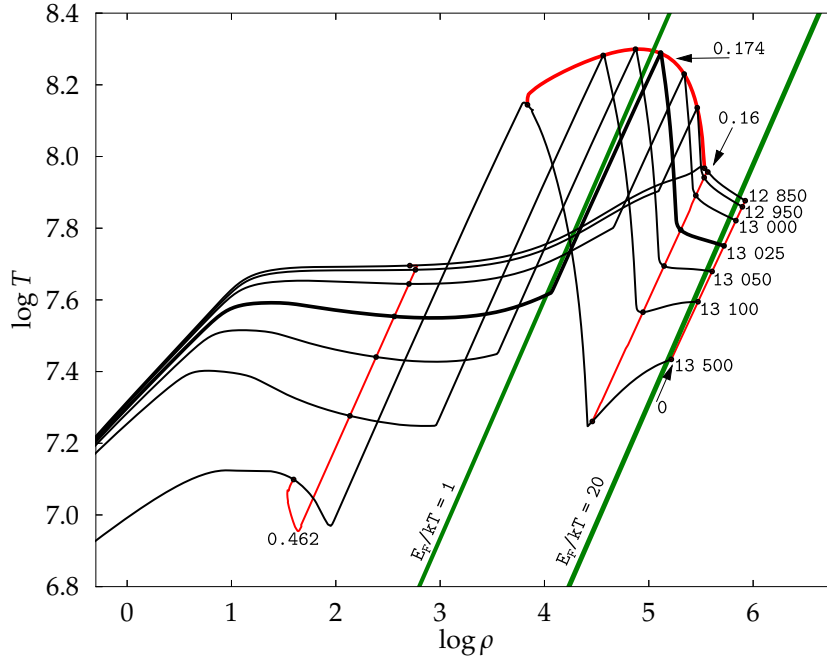


Figure 3: Loci on the $\log \rho - \log T$ plane of selected $1.3M_{\odot}$ models during the early initial He flash (model numbers from 12 850 to 13 500). The thicker black line marks the model during the peak of the initial helium flash. The red lines trace the evolution of a few mass shells (their mass depths are measured in solar-mass units) on the density - temperature plane. The heavier red line - at 0.174 - traces the locus of maximum ϵ_{nuc} of the helium burning shell during the early initial flash.

The green lines with $E_{\text{F}}/kT = 1$ and 20 illustrate lines of constant degeneracy. Since $E_{\text{F}} \sim \psi$, with E_{F} the Fermi energy and ψ the canonical degeneracy parameter, the low-order approximation of density in a strongly electron-degenerate environment reads $\rho \sim (\psi kT)^{3/2}$ so that $d \ln T / d \ln \rho|_{\psi=\text{const}} = 2/3$.

N.B. the black lines trace stratifications, i.e. the *spatial structure* of selected model stars; the red lines delineate *temporal*, lagrangian state changes along the sequence of stellar models.

vents the intershell convection zone to advance too far out. Under special conditions, which might not be realized in nature, a merging of convection zones could be enforced (Despain & Scalo 1976). Also, modeling the evolution of very low-metallicity (Pop III) stars revealed that ingestion of hydrogen into the He-burning shell during the onset of core helium burning can lead to enhanced convection zones in the core, due to the additional onset of hydrogen burning, so that eventually the deepening envelope convection zone can transport nuclearly processed material to the surface (e.g. Hollowell et al. 1990; Suda & Fujimoto 2010, and references therein). During even later evolutionary stages of any population-type star, the envelope convection zone usually overlaps temporally with regions containing matter that was previously modified by 3α burning and mixes it (2nd and 3rd dredge-up) into the superficial layers of red giants along the AGB.

Figure 4 shows Kippenhahn diagrams for nuclear and gravitational energy generation rates during the initial core helium flash. To provide a measure of the actual time evolution, epochs measured in years elapsed since initial flash peak at t_0 are given on top of the upper panel. The epoch of the second helium flash, at model 13 984, is denoted as $t_1 = t_0 + 185\,218$ yrs. The top panel depicts the behavior of the hydrogen-burning shell at fractional mass $q = 0.35$ and the helium-burning shell with its basis at $q = 0.13$. The hydrogen shell is, compared with the helium shell, very narrow in mass and goes es-

sentially extinct shortly after the initial flash but regains considerable strength after about 2000 yrs. Around minimum radius of the model star (model 13 833 at $t^* \approx 59\,400$ yrs) the hydrogen energy generation takes another dip because the radius of the H-shell grows and cools as it partakes in the expansion of the envelope towards the second thermal flash; shortly before the second flash, after the H-shell contracted and heated again, the hydrogen nuclear-energy generation regained its strength.

For a few years around the maximum of the initial flash, the helium-burning shell achieves a mass depth of about $0.13M_{\odot}$. From $t^* = 7$ yrs onward, the helium shell burns rather steadily but with a tendency to get weaker and thinner. The ‘gravitational energy generation rate’, $\varepsilon_{\text{grav}}$, shown in the lower panel is the temporal rate of change of the specific heat-content, Q , of the stellar material: $\partial_t Q = -\varepsilon_{\text{grav}}$. The locations of the helium- as well as hydrogen-burning shell are clearly discernible at about $q = 0.13$ and $q = 0.35$, respectively. The stellar core: the sphere interior to the He-shell does essentially not change its heat content, i.e. $\partial_t Q = 0$, during the initial flash, which means that state changes there are adiabatic (cf. red lines connecting e.g. $q = 0$ and $q = 0.16$ mass layers in Fig. 3).

The envelope above the H-shell shows signs of contraction (red) shortly after the initial He-flash when the intershell convection zone reaches its maximum extension and essentially quenches the H-shell. The intershell region is dominated by the convection zone induced by the He-burning shell. From the scale on the color bar in Fig. 3 we deduce that, centered around the initial flash, $\varepsilon_{\text{grav}}$ can easily compete in magnitude with the nuclear counterpart from 3α burning; this is the reason that stars with degenerate He-shell flashes are not disrupted by the enormous nuclear energy input; it is roughly balanced by decreasing the internal energy of the region and at the same time expanding it in the deep gravitational well of the star. The shape of the blue intershell region in the lower panel coincides with the extension of intershell convection zone. Since the convective time-scale is much shorter than the evolutionary time-scale after the flash peak, the rapid propagation of physical information throughout the intershell convection zone color along the q -axis (in particular before about model 13 600) levels out any developing $\varepsilon_{\text{grav}}$ gradient. The expansion of the envelope (above the H-shell) is visible as the blue channel leaving the plot on the upper right. On the other hand, the red region that establishes itself on top of the He-shell around model 13 400 and that continues to extend outwards, also crossing essentially unimpeded the H-shell before the second flash is dominated by an increase of the internal energy but not by volume work, i.e. by contraction.

The intershell convection zone of the $1.3M_{\odot}$ model sequence

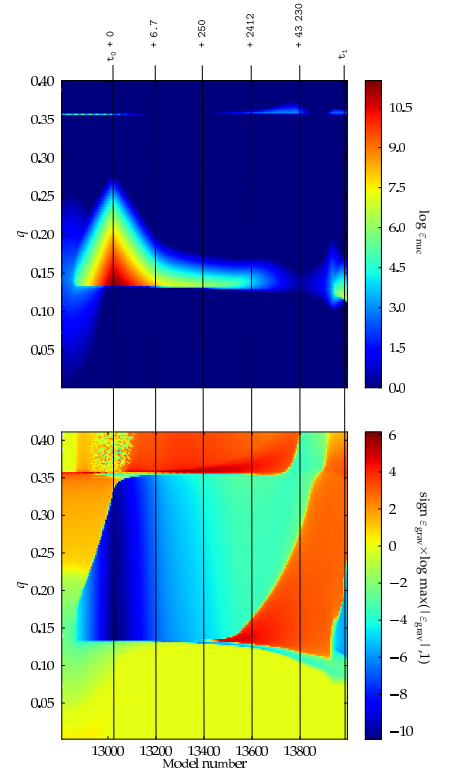


Figure 4: Color-coded Kippenhahn diagrams showing the energetics in the deep stellar interior during the initial helium flash, which is parameterized on abscissa with the model number; this choice accentuates the fast evolution during the flash peak. Physical times in years, relative to the epoch of the initial flash, t_0 , are overlaid over both panels. The epoch of the second helium flash is referred to as t_1 . The ordinates are chosen to be the fractional stellar mass q . The top panel shows the nuclear energy generation rate ε_{nuc} /erg/g/s and the lower panel a suitably transformed version of the gravitational energy generation $\varepsilon_{\text{grav}}$ /erg/g/s.

reaches its maximum extension at about model no. 13 200, i.e. at $t^* \approx 6.7$ yrs after initial flash peak and it dies out at $t^* \approx 3000$ yrs when 3α burning develops a local minimum after the central sphere below the helium-burning shell expanded and cooled adiabatically (see Figs. 4 and 5). The presence of the intershell convection zone causes the temperature gradient to be smoothed out, i.e. in the convection zone it is considerably shallower than on the radiative bottom-side of the He-burning shell (see model numbers $\geq 12\,950$ in Fig. 3); convection so deep in the stellar interior is essentially adiabatic so that the stratification is isentropic there.⁵ The steep temperature gradient on the bottom side of the helium-burning shell persists during the whole flash and is initially determined by the equation of state because the core cannot absorb any significant amount of energy during the flash. Since only very little mass is contained in the region of the sharp temperature drop (referred to as *temperature flank* in the following), the pressure gradient remains comparatively flat so that

$$\left| \frac{d \ln T}{dm} \right| \gg \left| \frac{d \ln P}{dm} \right|$$

obtains; the slope of the temperature flank on the $\rho - T$ plane can then be approximated by

$$\frac{d \ln T}{d \ln \rho} \approx \left(\frac{\partial \ln T}{\partial \ln \rho} \right)_P = -\frac{1}{\delta}.$$

Hence, the higher the degeneracy around the temperature maximum, the steeper the slope of the temperature flank. In the limit of nonrelativistic full degeneracy, the inner temperature flank is vertical in the $\log \rho - \log T$ plane.

During the early stage of the helium flash, the density of the core region of the star does not change noticeably; i.e. the heating due to the steeply increasing 3α energy generation does not inflict any significant expansion of the stellar material so that all liberated energy goes into further rising the local temperature at the nuclear burning shell. With increasing temperature in the flash region, electron degeneracy diminishes and in conjunction expansion can set in, i.e. an increasing fraction of the released nuclear energy goes into volume work and therefore less energy remains for further temperature rise. As an example: Since $\varepsilon_{3\alpha} \sim \rho^2 T^{41 \dots 19 \dots 12}$ at $T = 1 \dots 2 \dots 3 \cdot 10^8$ K, the rapid decrease of the temperature dependence of the energy generation rate with increasing temperature allows for an increasingly smaller density reaction to compensate the energy increase inflicted by some temperature rise: With the above numbers, the energy release produced by a relative temperature increase $\Delta T/T$ is neutralized by an associated relative density decrease of $\Delta \rho/\rho = 20.5 \dots 9.5 \dots 6 \cdot \Delta T/T$. Once such a limit is reached on the way of reducing the material's

⁵ Since $d \ln T / d \ln P = \nabla_{\text{ad}}$ obtains for the stratification, an ideal gas with negligible radiation pressure as well as a non-relativistic degenerate electron gas both support a slope

$$\left. \frac{d \ln T}{d \ln \rho} \right|_{\text{isent.}} = \frac{2}{3}.$$

The notation of physical quantities in this exposition is essentially that used in Kippenhahn & Weigert (1994); in particular the equation of state is assumed to be of the functional form: $\rho \sim P^\alpha T^{-\delta} \mu^\varphi$, with the characteristic exponents α, δ, φ .

degeneracy, the thermal flash has passed its maximum. In the $1.3M_{\odot}$ model sequence, this happens when the He-burning shell reaches the relatively high temperature of about $3 \cdot 10^8$ K, which lies already slightly below $E_F/kT = 1$ for model number 13 050 (see Fig. 3).

After the energy generation in the He-shell saturates, the size of the convection zone stalls too. The radiative regions overlying the convection zone cannot carry away the surplus energy since the evolution is still too rapid for diffusion to be effective. State changes in the layers above the adiabatically stratified intershell convection zone trace out loci with slopes very close to $2/3$ on the $\log \rho - \log T$ plane⁶ (see e.g. the state changes at $q = 0.462$ in Fig. 3). Only after about model number 13 400 enough time has elapsed for diffusion of radiation to influence state changes in the intershell region (see again the state change at mass shell $q = 0.462$ just before model 13 500 in Fig. 3) so that their loci on the $\log \rho - \log T$ deviate from lines with slope $2/3$.

The computations show that the expansion speed of the intershell region above the helium flash proceeds as $\partial_{mv} \approx \text{const.}$; using this in the continuity equation together with the assumption of adiabatic state changes, we find

$$\frac{\partial_t T}{T} \sim \frac{1}{r}.$$

Hence, in the inner parts of the radiative regions of the inter-shell layers cool stronger than the higher lying ones: This can be observed in Fig. 3 to the left of $E_F/kT = 1$, just outside of the intershell convection zone where a positive temperature gradient develops during the initial flash cycle.

In the degenerate core, state changes are also adiabatic (see lines of $q = 0$ and $q = 0.16$ in Fig. 3 or lower panel of Fig. 4). The expansion of the He-flash domain lifts its matter into regions of lower gravitational acceleration; hence, this expansion reduces the pressure on the inner core so that the very core expands adiabatically. Expansion is largest where degeneracy is lowest, i.e. around the He-flash shell. Due to near-adiabaticity of the state change, temperature change is biggest where expansion is biggest. Therefore, the originally slightly positive temperature gradient goes negative at the inner edge of the helium burning zone.

THE H-SHELL ESSENTIALLY SWITCHES OFF temporarily at about $t^* = 7$ yrs when the adiabatic expansion of the intershell region associated with the He-flash has sufficiently reduced the temperature at the H-shell. But only at $t^* \approx 44$ yrs has the surface luminosity dropped by $|\Delta L_*/L_*| = 0.1$ – this being taken as the sign that the star starts to leave the top of the giant branch at $2417 L_{\odot}$ (cf. column 4 in Table 1). At the end of the initial flash, the star’s luminosity reached $113 L_{\odot}$,

⁶ Introducing the constraint of an adiabatic state change

$$dQ = 0 = c_p dT - \frac{\delta}{\rho} dP$$

into the equation of state gives:

$$\left. \frac{d \ln T}{d \ln \rho} \right|_{dQ=0} = \frac{\nabla_{\text{ad}}}{\alpha - \nabla_{\text{ad}} \cdot \delta}.$$

Both cases of relevance here, the ideal gas with negligible radiation pressure with $\alpha = 1, \delta = 1, \nabla_{\text{ad}} = 2/5$ and the non-relativistic electron degeneracy with $\alpha = 3/5, \delta = 0, \nabla_{\text{ad}} = 2/5$, admit of

$$\left. \frac{d \ln T}{d \ln \rho} \right|_{dQ=0} = \frac{2}{3}.$$

which is roughly twice the luminosity at which it will finally settle to centrally burn helium. The core, being here the fractional stellar sphere lying inside of the H-shell, is hydrostatically insulated from the envelope, so that the core can change mechanically *without* dragging along the envelope (e.g. Stein 1966; Sugimoto & Nomoto 1980). Therefore, the delay of the surface luminosity reaction to what happens in the deep interior can be attributed to the Kelvin-Helmholtz time of the *radiative* intershell layers which must be overcome by photon diffusion. Once the envelope adjusts to the new energetic situation, the bottom of the envelope convection zone retreats. By $t^* = 2412$ yrs, i.e. model 13 600, helium burning eases off sufficiently for the He-shell convection zone to disappear (cf. Fig. 4). Around model number 13 740 ($t^* \approx 17650$ yrs), the first material layers of the contracting envelope hit and reflect on the steep density gradient at the H-burning shell. The generated ‘pulse’⁷ propagates back into the envelope and defines, upon its arrival at the stellar surface, the minimum radius and accordingly the minimum luminosity reached during the initial pulse ($47L_{\odot}$ at model no. 13 834, i.e. at $t^* \approx 62000$ yrs). The epoch of pulse generation at the H-shell goes along with a re-expansion and cooling of the H-shell and induces a phase of a nearly extinct hydrogen-burning shell. The spatial movement of the H-shell is reminiscent of a suction reaction inflicted by the rapid expansion of the overlying envelope. Meanwhile, the layers below the H-shell contract adiabatically (to rise density and temperature along loci of $d \ln T / d \ln \rho = 2/3$ – cf. Fig. 3) to eventually lead to the next thermal instability of the helium-burning shell.

The thermal pulsing episode of the helium shell

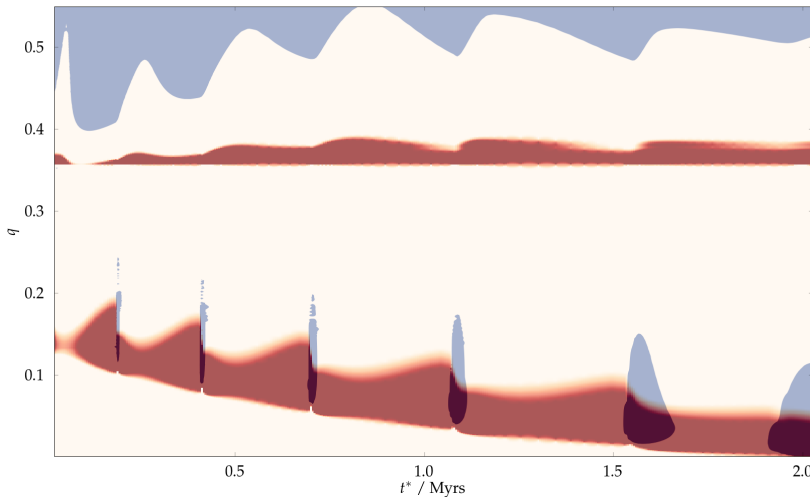
The initial helium flash is only the first of a series of flashes that accompany the inward burning of the He-shell toward the stellar center. Depending, among other parameters, on the stellar mass, the number of ensuing flashes can exceed a dozen at low stellar masses; the number goes down as the stellar mass increases and the initial flash takes place closer (measured in mass) to the stellar center. The physics of the thermal stability of thin nuclear-burning shells is well understood and documented e.g. in Kippenhahn & Weigert (1994). Most frequently, shell instability is encountered and studied in the evolution of stars along the asymptotic giant branch. The physics of the instability prevailing in the inward-burning He-shell at the onset of core helium burning of low-mass stars is, however, the same.

In all cases known to us, the first flash of the onset of helium burning in a low-mass star’s core is by a large margin the most energetic one. In the $1.3 M_{\odot}$ sequence exemplified here, the helium luminosity

⁷ The trace of the outgoing pulse is seen as the narrow blue locus close to the upper right corner of the plot on lower panel of Fig. 4.

grows to $10^{9.25}L_{\odot}$ during the initial flash. During the second flash, the helium luminosity is already about five orders of magnitude weaker with the tendency of a continuing weakening of the later flashes (see Fig. 8). The temporal evolution during the thermal pulsing phase of the nuclear burning ($\epsilon_{\text{nuc}} > 10 \text{ erg/g/s}$ plotted in red) in the stellar core is displayed in Fig. 5; the He-shell convection zone as well as the bottom of the envelope convection zone – both plotted in blue – are added for better orientation. The initial pulse (shown in an appropriately scaled way in Fig. 4) lies just off to the left of the diagram. Pulses two to six can be easily identified by the He-shell convection zone which they trigger.

The last pulse, which directly leads to sustained central helium burning is visible on the right of Fig. 5. The initial rise of helium burning looks like the previous *shell* instabilities; however, later during the flash, as the shell burns into the star’s center it can not react as before, the shell morphs into a central instability and hence into its rising the temperature at essentially constant density.



The innermost part of the envelope convection zone is visible along the top of the figure as the wavy blue band. The bottom of the convection zone reacts on the nuclear activity in the stellar core. Just as during the initial flash, also during the later ones the inner edge of the convective envelope recedes after each helium flash to re-penetrate deeper into the star during the later part of the thermal-pulse cycle. The bottom of the convective envelope never reached into material that was nuclearly processed during the thermal pulses so that there is, in our computations, no chance of dredging-up 3α burning products. While the helium shell burns its way into the stellar center on

Figure 5: Kippenhahn diagram for the inner 54% of the $1.3M_{\odot}$ model star’s mass, covering the end of the first (starting at model no. 13 400) and the ensuing five thermal flashes until central helium burning takes the star into a quasi-static state again. The time is measured in mega-years (Myrs) relative to t_0 . Regions with $\epsilon_{\text{nuc}} > 10 \text{ erg/g/s}$ are colored in red. Convective regions, as prevailing according to Schwarzschild’s criterion, are shaded in light blue. Notice that, according to our models, the bottom boundary of the envelope convection zone never penetrated deep enough into the star after the initial helium flash so that *no* dredge-up of 3α -processed material takes place.

The spotty character of the He-shell convection zone is spurious, caused by the Delaunay triangulation of strongly unequally spaced stellar-evolution data onto the regular grid that was computed for the color-coded plot.

the timescale of about 2 Myrs, the hydrogen shell remains essentially at constant mass depth. As can be deduced from Fig. 5, the H-burning shell reacts to the thermal pulsing He-shell by cyclically growing fatter shortly after each He-flash to later-on thin out again.

Figure 5 illustrates furthermore the regularity of the thermal flash cycles. As for the stars along the AGB, the time between two flashes, the interpulse period (IP), Δt_{IP} , appears to correlate with the core mass, m_c . For the $1.3M_{\odot}$ model sequence highlighted here, the core-mass – interpulse period relation is shown by dots in Fig. 6; they can be fitted by the relation

$$\log \Delta t_{\text{IP}} / \text{yrs} = 5.83 - 3.23 \left(\frac{m_c}{M_{\odot}} \right).$$

The core mass, m_c , was measured at the maximum of 3α burning, the interpulse period, Δt_{IP} , be the time passed between two He-flash peaks. The last point in the core-mass – interpulse-period diagram, i.e. the one belonging to the last helium flash, which started essentially centrally, was excluded from the analytical fit. The last flash is no longer pure in the sense that it is distorted by its proximity to the stellar center. Indeed, central burning evolves continually out of this distorted last flash. For comparison, the analytical fit to the interpulse-periods of the $0.6M_{\odot}$ models of Despain (1981) is shown as the continuous line in Fig. 6.

As the last helium flash ‘hits’ the star’s center, the 3α -burning matter cannot cool anymore by adiabatic expansion induced by the underlying material as hitherto, but it stays initially at roughly constant density while the temperature rises so that the material’s degeneracy is being reduced. Once degeneracy is low enough, the density starts to diminish. All this happens, as illustrated in Paxton et al. (2011), at essentially constant total pressure; this is achieved by the lack of any expansion/contraction of the material overlying the helium-burning core. Once, the stellar center’s degeneracy is lifted, central helium burning proceeds in complete equilibrium under essentially ideal-gas conditions.

THE MAJOR FEATURES OF THE WEDGE as traced out on the $\log \rho_c - \log T_c$ plane by a low-mass star’s center during the onset of core helium burning can eventually be understood qualitatively: In Fig. 7, epoch A indicates the tip of the first giant branch when the initial flash sets in. Epoch B marks the arrival of helium burning in the star’s center. Finally, state C is reached when the final thermal flash removes electron degeneracy in the center and quiescent *central* helium burning takes over. Notice that evolution of the star’s center from A to B on the $\log \rho_c - \log T_c$ does not proceed monotonously. During each thermal

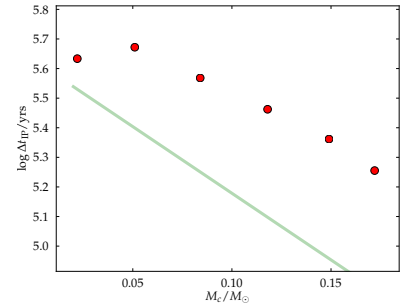


Figure 6: Interpulse-period – core-mass relation as observed in the evolution computations of the $1.3M_{\odot}$ models (red points), compared with the analytical fit by Despain (1981): $\log \Delta t_{\text{IP}} / \text{yrs} = 5.629 - 4.504 (m_c / M_{\odot})$ which is shown as full line in the figure.

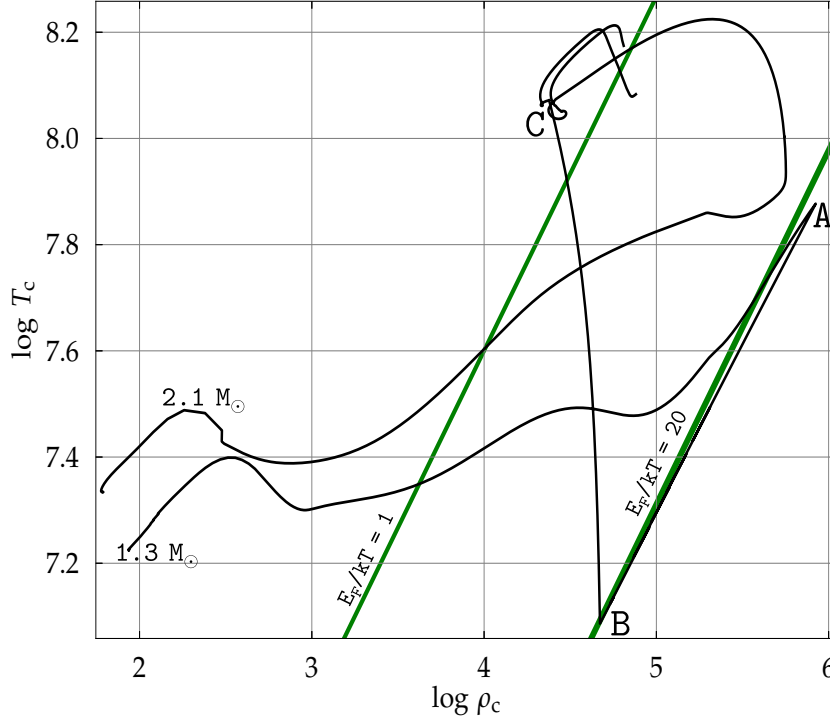


Figure 7: Evolution on the logarithmic density – temperature plane of the centers of the model stars shown in Fig.1. Epochs A, B, and C along the locus traced out by the center of the $1.3 M_{\odot}$ model star define the edges of the ‘wedge’, which is referred to in the text. In the case of the $2.1 M_{\odot}$ star whose helium burning starts in the center, the corresponding density stays initially essentially constant but the temperature rises strongly and maneuvers the star’s center out of degeneracy already during the initial flash.

flash the star’s center moves back and forth along a locus of essentially $E_F/kT = \text{const.}$; the magnitude of E_F/kT which prevails in a star’s center remains essentially constant, determined by the total stellar mass. During the luminosity decline of each pulse cycle, the central density (and temperature) decline; during the ascending phases the cycles, luminosity and central density (and also temperature) rise again slightly. The magnitudes of the density rises are smaller than the cyclic declines, so that an effective reduction in central density and temperature result throughout the flash cycles. The fact that degeneracy of the stellar center does hardly change during the series of thermal pulses is attributable to lines of constant degeneracy and loci traced out by adiabatic state changes, both having the same slope.

EVEN THOUGH THE HELIUM LUMINOSITY DOMINATES early phases of the initial flash cycle, other components, usually not being in the limelight of attention, affect the star’s luminosity once the thermal instability of the helium shell fades away. Figure 8 shows that it is the gravitational luminosity⁸, L_g , which dominates all other luminosity contributions (except for L_{He} during the short flash peaks) for the first roughly 1 Myr after the initial flash; during this phase, the $1.3 M_{\odot}$ star evolves from the tip of the giant branch to its clump position at about $60 L_{\odot}$. The gravitational luminosity takes over the rôle of the dominant

⁸ The casually referred to *gravitational luminosity* is defined as

$$L_g \doteq \int \epsilon_{\text{grav}} dm;$$

it is a measure of a star’s departure from thermal equilibrium.

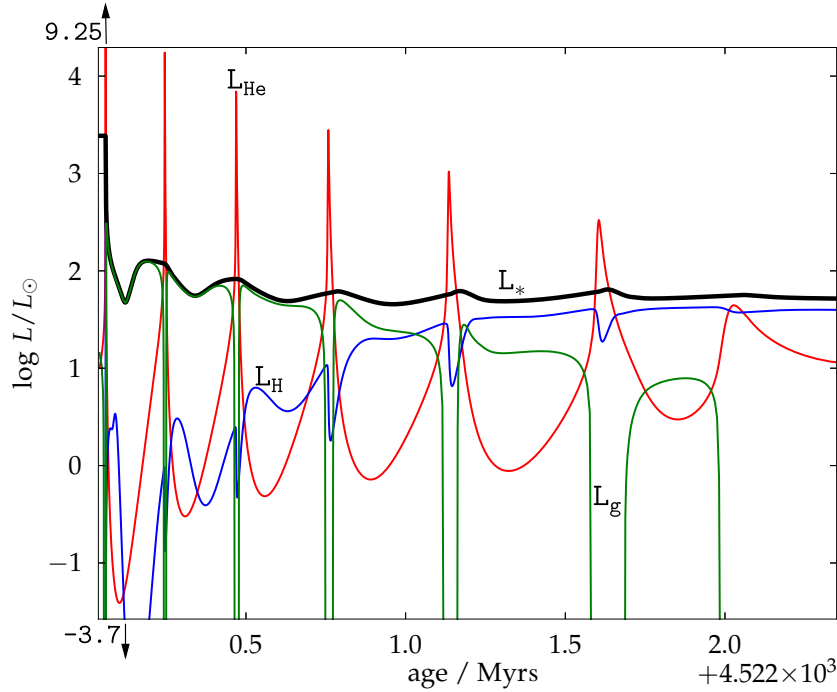


Figure 8: Evolution of the total stellar luminosity (L_* , heavy line) and its constituent components, luminosity from hydrogen burning (L_H), luminosity from helium burning (L_{He}), and the ‘gravitational luminosity’ (L_g) during the onset of helium burning in the $1.3M_\odot$ star model.

luminosity source at around $t^* = 2400$ yrs, after the L_H minimum passed and the envelope shrunk from 160 to $43R_\odot$. During this later phase of the initial pulse cycle it is the envelope above the H-burning shell that contributes most to L_g . The biggest positive L_g contribution comes from the very base of the envelope, the region closest to the H-burning shell, which lies also in the steepest part of the gravitational potential.⁹ The L_g behavior during the subsequent flashes, with successively lower amplitude and with accordingly smaller radius and thermal variation, is qualitatively the same as that during the initial He-flash cycle.

After the initial flash, the hydrogen shell dims out so that at model 13 200 (i.e. at $t^* = 6.7$ yrs) it reaches a minimum at $L_H = 10^{-3.7}L_\odot$ as also seen in Fig. 4. Figure 8, on the other hand, shows the hydrogen shell to regain sufficient strength after the forth pulse and overtaking L_g ; the hydrogen-luminosity continues to grow and finally takes over as the dominant nuclear energy source of the star during the ensuing inter-flash phases. Even after central helium burning is established, the H-shell retains the status as the dominant nuclear energy source. At most, the 3α luminosity exceeds the H-luminosity by 35 % during the initial peak of central helium burning, but most of the time it is clearly superseded by the energy output of the H-burning shell.¹⁰

During the whole thermal-pulse phase, however, $\varepsilon_{\text{grav}} \approx 0$ obtains

⁹ The thermal time-scale ($\int c_V T dm / L_*$) of the envelope, extending from the photosphere to the outer edge of the H-burning shell, computed for the conditions at the tip of the red-giant branch amounts to a few hundred years. Only when assuming the envelope to encompass also the intershell region could the corresponding thermal heat content power the star for about 10^4 yrs.

¹⁰ $L_H/L_{He} = 2.4 - 3.4$ during most of the central He-burning.

in the central sphere bounded by the He-shell, i.e. it stays inert in every energetic respect. It is the diffusion time-scale of the He-burning shell into this inert degenerate central sphere which determines the duration of the thermal pulsing phase. Analytical guesswork is cumbersome due to the rather strong variation of the pertinent physical quantities at the He-burning shell during the flash cycles; depending on the particular choices, durations between 10^5 and 10^7 yrs result; stellar evolution computations yield 2×10^6 yrs.

OFF-CENTER HELIUM FLASHES burn some of the helium (see Fig. 9) mainly to carbon and oxygen so that heavier material overlies lighter one in the core – a potentially unstable situation. Since stellar material is not isothermal in the relevant regions, the stratification is not just Rayleigh-Taylor unstable; the prevailing temperature profile can stabilize a certain magnitude of molecular-weight contrast. The non-vanishing diffusivity of heat requires then the stability condition against double-diffusive mixing to be studied.¹¹ Even though the qualitative picture of the onset of core-helium burning as observed through the results from stellar structure and evolution computations¹² seems to be robust, any quantitative study requesting information on abundances and abundance profiles, either as observed directly on red-giants' surfaces or possibly deduced via observed oscillation frequencies of red giants will require detailed multi-dimensional CFD simulations of the stellar core region. The same applies to the study of the detailed influence of the dynamical convection and what happens at the corresponding convective boundaries at the He-burning shell during the initial flash.

ACKNOWLEDGMENT NASA's Astrophysics Data System was used extensively for this exposition. Without the open-source project MESA, none of the illustrations and analyses presented in this paper would have been possible; the efforts and willingness to communicate, in particular of the 'chief developer', Bill Paxton, are highly appreciated and equally admired. I am grateful to Hideyuki Saio who helped to improve the content of this exposition by critically commenting on the typescript. H. Harzenmoser stimulated and followed closely also this project; he tried to keep up the author's spirits during numerous culinary late-night sit-ins that reverberated from exegeses on the virtues of fostering understanding rather than aggregating yet more information.

References

Bedding, T. R., Mosser, B., Huber, D., et al. 2011, *Nature*, 471, 608

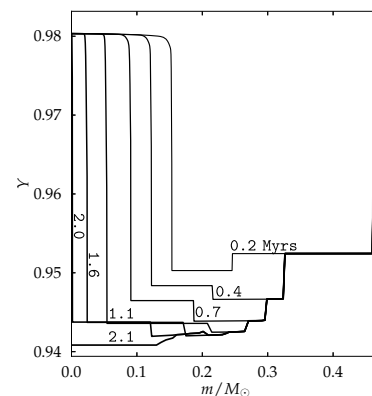


Figure 9: Spatial variation of the helium abundance in the cores of $1.3M_{\odot}$ models. The epochs of the snapshots, measured in Myrs as relative times t^* , are labeled on the respective profiles. The lowest six epochs were chosen at the local minima of L_{He} between the thermal pulses. At $t^* = 2.1$ Myrs, central helium burning was already in progress.

¹¹ This is the same physical phenomenon as the salinity steps observed in the stratification of sea water observable at favorable places on the globe. Therefore, even in highly compressible stellar astrophysics, this double-diffusive instability is mostly referred to as salt-finger or thermohaline instability – the names used in oceanography.

¹² Essentially measured heuristically by comparing the results of different generations of stellar-evolution codes, all with different micro-physics and many of them with different numerics.

- Bildsten, L., Paxton, B., Moore, K., & Macias, P. J. 2012, *ApJ*, 744, L6
- Demarque, P. & Mengel, J. G. 1971, *ApJ*, 164, 317
- Despain, K. H. 1981, *ApJ*, 251, 639
- Despain, K. H. & Scalo, J. M. 1976, *ApJ*, 208, 789
- Härm, R. & Schwarzschild, M. 1964, *ApJ*, 139, 594
- Hollowell, D., Iben, I., & Fujimoto, M. Y. 1990, *ApJ*, 351, 245
- Iben, I. 1974, *ARAA*, 12, 215
- Kippenhahn, R. & Weigert, A. 1994, *Stellar Structure and Evolution* (Springer)
- Mengel, J. G. & Sweigart, A. V. 1981, in *IAU Coll. 68, Astrophysical Parameters for Globular Clusters*, ed. A. Davies & D. Hayes (L. Davies Press, Schenectady), 277
- Mocák, M., Meakin, C. A., Müller, E., & Siess, L. 2011, *ApJ*, 743, 55
- Paxton, B., Bildsten, L., Dotter, A., et al. 2011, *ApJS*, 192, 3
- Salaris, M. & Cassisi, S. 2005, *Evolution of stars and stellar populations* (Wiley)
- Serenelli, A. & Weiss, A. 2005, *A&A*, 442, 1041
- Stein, R. 1966, in *Stellar Evolution*, ed. R. Stein & A. Cameron (Plenum Press), 3
- Suda, T. & Fujimoto, M. Y. 2010, *MNRAS*, 405, 177
- Sugimoto, D. & Nomoto, K. 1980, *SSRv*, 25, 155
- Thomas, H. 1967, *ZfA*, 67, 420